Hysteresis-Free Blue Phase Liquid-Crystal-Stabilized by ZnS Nanoparticles

Ling Wang, Wanli He,* Xia Xiao, Fanguo Meng, Yang Zhang, Pangyen Yang, Liping Wang, Jiumei Xiao, Huai Yang,* and Yunfeng Lu*

Liquid-crystalline blue phases (BPs) have sparked an enormous interest due to their exotic optical properties, exhibiting no birefringence but selective reflection of circularly polarized light, and potential for advanced applications in a wide variety of fields including self-assembling tunable photonic crystals and fast-response display.[1] BPs are made up of double-twist cylinders arranged in a highly fluid self-assembled cubic lattice with periods of ~100 nm, which is stabilized by a network of topological –1/2 disclination lines. The competition between the chiral forces and the packing topology leads to at least three different lattice structures, labeled as blue phase III (BPIII), blue phase II (BPII), and blue phase I (BPI) upon decreasing the temperature from the isotropic (I) to the chiral nematic phase.[2] The packing structures are macroscopically amorphous, simple cubic, and body-centered cubic, respectively.[3] As is known, the main obstacles to the potential applications of the BPs are the narrow temperature range as well as the instability of cubic structure against an electric field.[4] Recent developments that introduce BPs with an extended temperature range[5] make them more attractive for applications. However, the stability of cubic structures against an electric field, such as heavy hysteresis or irreversible switching, is still a big challenge on the road toward practical applications.

Theoretical investigations of the BP switching dynamics in presence of an electric field have shown that cubic structure (especially, BPI) is unstable and difficult to be reversibly switched in the strong field region.[6] It has been experimentally demonstrated that serious hysteresis was observed in the pure BPs, which may be due to the field induced phase transition from BP to a chiral nematic phase.[7] Interestingly, polymer-stabilized BPs (PSBP) could be reversibly switched with microsecond response time,[5] but the driving voltage of these system is relatively high due to the doping of ~10.0 wt% monomers, and the long-term stability of polymer network is a remaining technical challenge.[1,8] Moreover, BPIII could also undergo a reversible switching with an AC field of less than 10.0 V μm^{-1} but the response speed is relatively slow (about several millisecond) due to the fact that BPIII with wide temperature range is usually observed in the systems with high chirality or viscosity.[9] Therefore, there is an urgent need to explore a novel strategy to solve the instability of cubic BPs against an electric field and develop the BP composites without hysteresis, with fast response speed, and with low driving voltage.

Liquid-crystal nanoscience has attracted special attention in recent years due to the potential applications in developing new composite materials with exciting optical as well as electro-optical properties.[10] Doping nematic liquid crystals (LC) with nanoparticles (NPs) has lead to many promising LC electro-optical characteristics including low driving voltages,[11] short response time,[12] frequency modulation response,[13] and memory effect.[14] In particular, suspensions of NPs in BPs were believed to replace part of the energetically costly disclination region with the particles' own volume, lowering the overall energy of the LC texture, consequently enhancing the stability of BPs.[5,15] Herein, we firstly report another exciting phenomenon in the nanoparticle-stabilized BPs: a reversible electro-optical switching like PSBP could be achieved in a BPI dispersed by a small amount of ZnS NPs; the on-state voltage is much lower than that of PSBP, and the hysteresis is so small that it can be considered as hysteresis-free at a 0.5–0.7 wt% doping level. These studies will certainly provide a simple and effective method to improve the electro-optical (E-O) performances of the new promising BP liquid-crystal displays (LCDs).

L. Wang, Dr. W. He, F. Meng, Y. Zhang, L. Wang, J. Xiao, Prof. H. Yang, Prof. Y. Lu
Department of Materials Physics and Chemistry
University of Science and Technology Beijing
Beijing 100083, P. R. China
E-mail: hewanli@mater.ustb.edu.cn;
yanghuai@mater.ustb.edu.cn; yanghuai@coe.pku.edu.cn;
luucla@ucla.edu

X. Xiao, Dr. P. Yang
AU Optronics Trade (Shanghai) Corporation
Suzhou 215021, P. R. China

Prof. H. Yang
Department of Materials Science and Technology
College of Engineering
Peking University
Beijing 100871, P. R. China

Prof. Y. Lu
Department of Chemical and Biomolecular Engineering
University of California
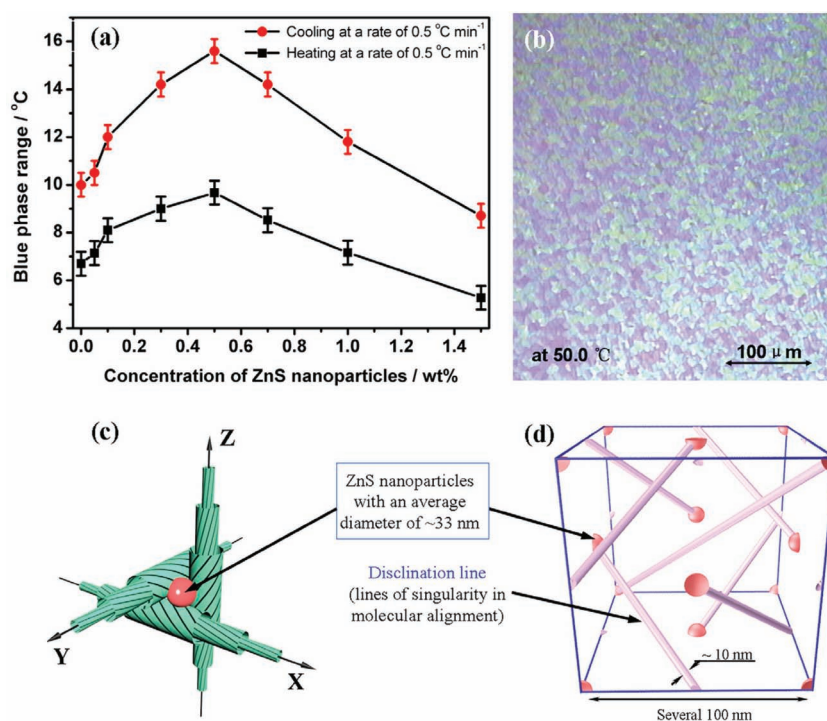Los Angeles, CA 90095, USA

Figure 1. a) Effect of the concentration of ZnS NPs on the blue-phase range of liquid-crystalline composites. b) POM photos of the natural textures of BPI stabilized by 0.5 wt% ZnS NPs on cooling. c) The disclination core between the double-twisted cylinders filled with ZnS NPs. d) The disclination lattices of BPI stabilized by the ZnS NPs.

The hydrophobic surface-treated ZnS NPs with an average diameter of ~33 nm were prepared by a simple reverse micelle reaction involving polyoxyethylene octyl phenyl ether (Triton X-100) as a surfactant, which has been previously reported in our work.[16] And the BPI-exhibiting LC material was a mixture comprising the following materials: SLC-X (82.0 wt%, Yongsheng Huatsing Liquid Crystal Co., Ltd, birefringence: $\Delta n = 0.235$, dielectric anisotropy: $\Delta \varepsilon = 29.6$ at 298 K), R811 (10.0 wt%, Merck) and Iso-(6OBA)$_2$ as that used previously [5c] (8.0 wt%, synthesized in our laboratory). The liquid-crystalline composites doped with different concentration of ZnS NPs were prepared by dispersing the NPs into the BPI-exhibiting LC material (see Experimental Section: *Preparation of samples*), and their actual phase transition temperatures were listed in Table S1 (see Supporting Information (SI)). As is shown in **Figure 1**a, when doped with ZnS NPs ranging from 0.05 to 0.5 wt%, the mixtures show an increasing BPI range with the widest to 15.6 °C, whereas further addition of the NPs suppresses the range. Furthermore, BPI ranges of the heating process are 30–40% narrower than those of the cooling process, which may be due to the supercooling of BPI in the case of cooling. Figure 1b indicates the typical textures of BPI doped with 0.5 wt% ZnS NPs, which was taken by using a polarized optical microscope (POM).

The stability of BPs depends on a well-arranged double-twisted alignment and a stable defect.[3] According to the defect theory, the free energy around defects decreases on the introduction of surface elasticity.[17] Additionally, it has been demonstrated that BPs can be stabilized by removing part of the volume occupied by the disclination lines, and

replacing it with non-LC materials, such as polymers.[5,18] Theoretical simulation has found that nanoparticles doped in BPs will most likely be trapped in the disclination lines as a result of elastic interactions.[19] Therefore, we could infer that the initially freely moving NPs became trapped once they met a disclination line, and that the volume and the free energy around the disclination were consequently reduced. A possible mechanism for the BPI stabilized by ZnS NPs with an average diameter of ~33 nm can be depicted as in Figure 1c,d, which individually indicates that the disclination core between the double-twisted cylinders was filled with ZnS NPs, and the disclination lattice of BPI was stabilized by the NPs. The volume and the free energy around the disclinations could be continuously suppressed with increasing the concentration of ZnS NPs, but the cubic structures of BPI would be disordered after the critical concentration had been reached. The above viewpoint may be a possible interpretation for the effect of the concentration of ZnS NPs on the BP range of the composites.

Macroscopically, BPLC is an isotropic Kerr medium when there is no external electric field (E) present. As E increases, the BPLC becomes anisotropic along the electric field direction, and the change of the refractive index follows the Kerr effect in the low field region but gradually saturates as the electric field keeps increasing, which can be well explained by an extended Kerr effect.[20] Based on the Kerr effect, the induced birefringence $\Delta n_{\text{induced}}$ in the weak field region is related to E, wavelength λ, and Kerr constant K as:[21]

$$\Delta n_{\text{induced}} = \lambda K E^2 \tag{1}$$

NP–LC composites have been previously utilized in the devices with reduced threshold voltage and much better optical contrast. In order to make an intensive research on the influence of ZnS NPs on the E-O performances of BPI, the E-O effects in the BPI-exhibiting composites stabilized by different concentration of ZnS NPs were investigated in detail by incorporating in-plane electric field geometry (see Experimental Section: *Measurement*).

Figure 2a shows the voltage–transmittance curve of the composites as a function of applied AC rectangular voltage of 60 Hz at the reduced temperature T, $T_{\text{I-BP}} - T = 6.0$ °C. Herein, transmittance with 0% was calibrated by that of the cell under crossed polarizers; the present actural optical transmittances are relatively low due to the fact that the detected transmittance was only 35.0% under parallel polarizers. The BPI of the mixture without ZnS NPs was difficult to reverse back to the original state after the peak transmittance had been reached, whereas it could be found that the hysteresis effects would be markedly overcome in the samples blended with a proper quantity of ZnS NPs.
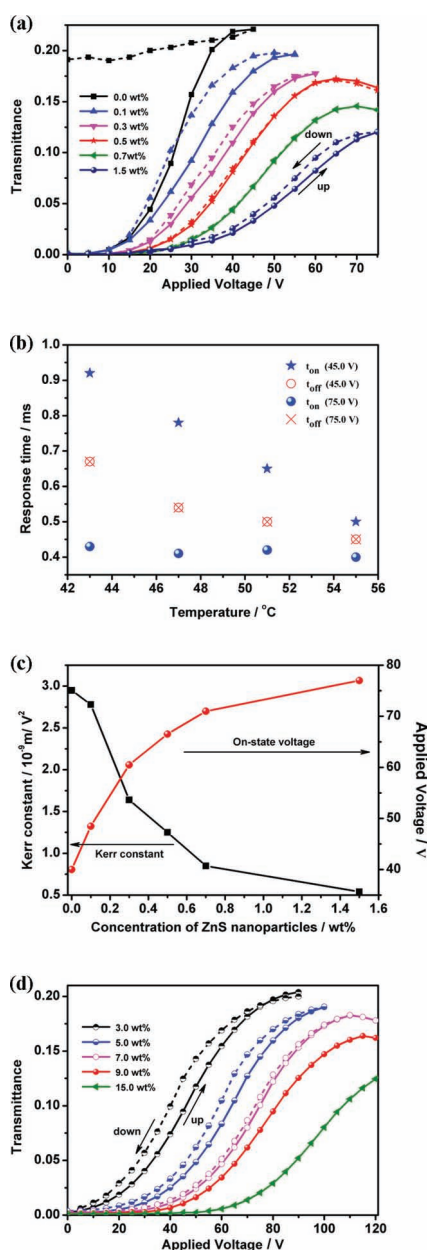
Figure 2. a) Voltage–transmittance curve of the BPI-exhibiting composites stabilized by different concentration of ZnS NPs as a function of applied AC rectangular voltage of 60 Hz. b) Temperature dependence of the response times for the rise and decay processes in BPI stabilized by 0.7 wt% ZnS NPs with different AC voltage at 60 Hz. c) Kerr constants and on-state voltage (V_{on}, corresponding to the peak transmittance) for the BPI as a function of the concentration of ZnS NPs, measured at the reduced temperature T, $T_{I-BP} - T = 6.0$ °C. d) Voltage–transmittance curve of PSBP with different concentration of monomers as a function of applied AC rectangular voltage of 60 Hz.

To measure the hysteresis, we drive the in-plane-switching (IPS) devices by ascending the voltage to on-state voltage (V_{on}, corresponding to the voltage of peak transmittance). Hysteresis is defined as $\Delta V/V_{on}$, where ΔV is the difference of the voltage between the forward and backward scans at half of the peak transmittance.[22] Surprisingly, the composite doped with only 0.1 wt% ZnS NPs could reverse back to the original state in despite of the relatively high hysteresis

(12.7%), whereas the samples with the NPs ranging from 0.3 wt% to 0.5 wt% show a decreasing hysteresis (from 2.6% to 0.4%). Particularly, the almost hysteresis-free E-O switching behaviors were observed in the liquid-crystalline composites doped with 0.7 wt% ZnS NPs, where the hysteresis is so small that it can be considered as hysteresis-free. However, further addition of the NPs amplified the hysteresis loop and suppressed the peak transmittance, which may be resulted from the fact that the cubic structures of BPI would be disordered when doping the excessive amount of the NPs. Figure 2b shows the temperature dependence of the response times for the rise and decay processes in BPI stabilized by 0.7 wt% ZnS NPs with different AC voltage at 60 Hz. As is shown, the rise time (t_{on}) was found to increase concomitantly with the decreased voltage, whereas the decay time (t_{off}) was found to be independent of the voltage. With an AC voltage of 75.0 V, the rise time is independent of the temperature, although the decay time lengthens with decreasing temperature; in contrast, the rise time lengthens with decreasing temperature under an AC voltage of 45.0 V. Figure 2c portrays the Kerr constant and V_{on} for the BPI as a function of the concentration of ZnS NPs. It is clear that the Kerr constant decreased and V_{on} increased with increasing the concentration of ZnS NPs. Moreover, the magnitude of the Kerr constant at the BPI state is almost 1000 times greater than that of conventional Kerr materials such as nitrobenzene ($K = 2.2 \times 10^{-12}$ mV^{-2}). Increasing the concentration of ZnS NPs might enhance the anchoring of LC molecules around the NPs, and a larger voltage would be required to reorient LC along the direction of the applied electric field, consequently increasing the on-state voltage V_{on}. In addition, the decreased Kerr constant may be due to the fact that the elastic constant k would be increased with the increasing concentration of the NPs.

It must be mentioned that theoretical simulations have shown that BPI can not get back to its original defect structure due to the fact that the cubic structure is permanently deformed under the large electric field.[6b] To our surprise, reversible E-O switching was observed in BPI stabilized by doping a small amount of ZnS NPs. As shown in **Figure 3**, a dark state was obtained at the optically isotropic BPI
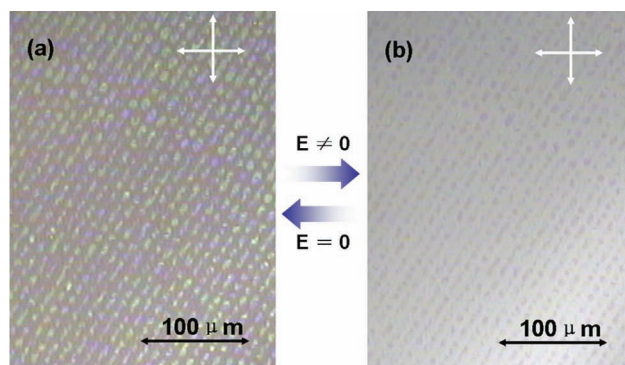

Figure 3. POM photos of the BPI stabilized by 0.7 wt% ZnS NPs under the in-plane electric field geometry a) without the applied voltage and b) with the applied voltage of 75.0 V. The crossed arrows indicate the directions of the polarizers.

state in the absence of the electric field, whereas a bright state could be observed under the applied voltage of 75.0 V. Additionally, the BPI could still reverse back to its original state after several switching circles, and both the rise time and the decay time of the samples were less than 1 ms. As is known, the switching behaviors of the cubic BPs are intimately interconnected with the dynamics of the disclination network constituting these phases.[6a] The liquid-crystalline texture and disclination pattern may be pinned at least partially by impurities or it may be kept for some time due to surface "memory" effects which slow down the dynamics close to the boundaries. When the electric field is applied, the network breaks down and then the disclinations pin to the boundaries.[23] In the case of our BPI devices, we could infer that the introduction of ZnS NPs, on the one hand, suppressed the volume of the disclination region, enhancing the stability of BPs; on the other hand, introduced new boundaries or impurities into LC, pinning the disclination pattern of BPI and improving the regrowth speed of the disclination pattern after the electric field being switched off. The strong elastic interactions between the disclination and the NPs may be the reason for reversible switching of the BPI.

In order to make an intensive comparison with the PSBP, we studied the E-O performances of the BPI stabilized by two kinds of polymerisable acrylate monomers: a di-functional monomer C6M and a tri-functional monomer TMPTA (see SI). The weight ratio of the monomers was fixed at 5/4, and the overall monomer concentrations were controlled ranging from 3.0 to 15.0 wt%. As shown in Figure 2d, V_{on} increases with increasing the concentration of the monomers, and the samples with 3.0 and 5.0 wt% monomers have the V_{on} of less than 80.0 V but serious hysteresis is observed. Moreover, the hysteresis is relatively small and can be considered as hysteresis-free in the samples stabilized by more than 9.0 wt% monomers, but the V_{on} is so high (>100.0 V). In comparison, reversible switching without hysteresis can be also achieved by the suspensions of ZnS NPs at a 0.5–0.7 wt% level. Significantly, the V_{on} is much lower than that of PSBP, which could be attributed to larger dipole moment of the NPs that enhances the anchoring of LC molecules around ZnS NPs.[24]

In summary, the reversible E-O switching was facilely achieved in the BPI stabilized by a small amount of hydrophobic surface-treated ZnS NPs with an average diameter of ~33 nm, the hysteresis is so small that it can be considered as hysteresis-free at a 0.5–0.7 wt% doping level, and the V_{on} is much lower than that of PSBP, in which the strong elastic interactions between the disclination and the NPs were believed to play an important role. Furthermore, the range of the nanoparticle-stabilized BPI was also extended even up to about 15.6 °C, which is thought to originate from the fact that the volume and the free energy around the disclinations were suppressed by introducing the NPs. Our observations are expected to pave way for developing the BP composites that exhibit low driving voltage, wide temperature range, and good stability against an electric field, leading to the potential applications in areas of display as well as optoelectronic devices.

Experimental Section

Preparation of Nanoparticles: ZnS NPs were synthesized in reversed micelle following standard procedures with a slight revision, using Triton X-100 as a surfactant. The preparation was carried out by mixing two reverse micellar solutions with the same water-to-surfactant molar ratio (W_o = [W]/[S]) containing the same concentration of Zn^{2+} or thioacetamide. To make a stable reverse micelle, a solution of $ZnAc_2 \cdot 2H_2O$ or thioacetamide was added into a mixture of cyclohexane and Triton X-100, followed by dropwisely adding a small amount of n-butanol as a co-surfactant under stirring. After the mixture became clear, a 1:1 molar ratio of zinc-ion-containing micelle mixed with sulfur-containing micelle, stirred with the aid of ultrasound for the desired time, yields a yellowish emulsion. The X-ray diffraction (XRD) spectrum and transmission electron microscopy (TEM) image of the ZnS NPs were shown previously.[17]

Preparation of Samples: The BPI-exhibiting LC material (BPLC) was a mixture comprising the following materials: SLC-X (82.0 wt%, Yongsheng Huatsing Liquid Crystal Co., Ltd, Δn = 0.235, $\Delta \varepsilon$ = 29.6 at 298 K), R811 (10.0 wt%, Merck) and Iso-(6OBA)$_2$ (8.0 wt%, synthesized by our laboratory). And the liquid-crystalline composites doped with different concentration of ZnS NPs were prepared by dispersing the NPs into BPLC. In order to achieve good dispersion, the mixtures of BPLC with ZnS NPs were dissolved in acetone and sonicated for about 1.0 h. Then, acetone was evaporated off slowly for about 24 h above 45 °C before the samples were placed in a vacuum system at 1023 Torr for 24 h at 50 °C.

Measurements: The phase transition temperatures and the natural textures of BPI for the liquid-crystalline composites were achieved by using the thermal optical microscopy with a polarizing microscope (Olympus BX-51) equipped with a Linkam Scientific LTS 350 heating/freezing stage. Optical transmittance was observed for a sample contained in the region between the comb-type interdigitated electrodes under the crossed polarizers, as a function of applied AC rectangular voltage of 60 Hz. The samples in the in-plane-switching (IPS) cells were placed at an inclination angle θ of 45° with respect to incident light, and the temperature was controlled with a hot stage calibrated to an accuracy of ±0.1 °C (Linkam LK-600PM). The IPS cells were kindly supplied by AU Optronics Corporation, and the indium tin oxide electrode width was 5.0 μm, the distance between the electrodes was 5.0 μm, and the cell gap was maintained at 10.0 μm by spacers. The response time for the rise process is defined as t_{0-90} (t_{on}), which is the time for the increase in the transmittance from the initial state to 90% of the saturated state. That for the decay process is defined as t_{100-10} (t_{off}), which is the time for the decrease in the transmittance from the initial state to 10% of the saturated state.

Supporting Information

Supporting Information is available from the Wiley Online Library or from the author.

Acknowledgements

[1] a) W. Cao, A. Munoz, P. Palffy-Muhoray, B. Taheri, *Nat. Mater.* **2002**, *1*, 111; b) J. Yan, L. Rao, M. Jiao, H. C. Cheng, S. T. Wu, *J. Mater. Chem.* **2011**, *21*, 7870.

[2] P. Crooker, *in Chirality in Liquid Crystals* (Ed: H.-S. Kitzerow, C. Bahr), Springer, New York, **2001**.

[3] H. Kikuchi, *Struct. Bonding* **2008**, *128*, 99.

[4] a) S. Meiboom, M. Sammon, W. F. Brinkman, *Phys. Rev. A.* **1983**, *27*, 1438; b) J. P. Sethna, D. C. Wright, D. N. Mermin, *Phys. Rev. Lett.* **1983**, *51*, 6467; c) D. C. Wright, N. D. Mermin, *Rev. Mod. Phys.* **1989**, *61*, 385; d) E. Karatairi, B. Rozic, Z. Kutnjak, V. Tzitzios, G. Nounesis, G. Cordoyiannis, C. Glorieux, J. Thoen, S. Kralj, *Phys. Rev. E.* **2010**, *81*, 041703.

[5] a) W. He, G. Pan, Z. Yang, D. Zhao, G. Niu, W. Huang, X. Yuan, J. Guo, H. Cao, H. Yang, *Adv. Mater.* **2009**, *21*, 2050; b) H. Yoshida, Y. Tanaka, K. Kawamoto, H. Kubo, T. Tsuda, A. Fujii, S. Kuwabata, H. Kikuchi, M. Ozaki, *Appl. Phys. Express* **2009**, *2*, 121501; c) H. Coles, M. Pivnenko, *Nature* **2005**, *436*, 997; d) H. Kikuchi, M. Yokota, Y. Hisakado, H. Yang, T. Kajikawa, *Nat. Mater.* **2002**, *1*, 64; e) Y. Chen, J. Yan, J. Sun, S. T. Wu, X. Liang, S. H. Liu, P. J. Hsieh, K. L. Cheng, J. W. Shiu, *Appl. Phys. Lett.* **2011**, *99*, 201105.

[6] a) G. P. Alexander, D. Marenduzzo, *EPL.* **2008**, *81*, 66004; b) A. Tiribocchi, G. Gonnella, D. Marenduzzo, E. Orlandini, *Soft Matter* **2011**, *7*, 3295.

[7] a) H. Choi, H. Higuchi, H. Kikuchi, *Appl. Phys. Lett.* **2011**, *98*, 131905; b) L. Wang, W. He, X. Xiao, Q. Yang, B. Li, P. Yang, H. Yang, *J. Mater. Chem.* **2012**, *22*, 2383.

[8] L. Rao, J. Yan, S. T. Wu, *J. Soc. Info. Display* **2010**, *18*, 954.

[9] a) M. Sato, A. Yoshizawa, *Adv. Mater.* **2007**, *19*, 4145; b) A. Yoshizawa, Y. Kogawa, K. Kobayashi, J. Yamamoto, *J. Mater. Chem.* **2009**, *19*, 5759; c) S. Taushanoff, K. V. Le, J. Williams, R. J. Twieg, B. K. Sadashiva, H. Takezoe, A. Jakli, *J. Mater. Chem.*

[10] a) H. Qi, T. Hegmann. *J. Mater. Chem.* **2008**, *18*, 3288; b) H. K. Bisoyi, S. Kumar, *Chem. Soc. Rev.* **2011**, *40*, 306.

[11] S. Kaur, S. P. Singh, A. M. Biradar, A. Choudhary, K. Sreenivas, *Appl. Phys. Lett.* **2007**, *91*, 023120.

[12] B. F. Li, B. Huang, X. K. Ding, W. B. Li, Y. H. Yin, L. P. Wang, H. Cao, H. Yang, *Liq. Cryst.* **2008**, *35*, 49.

[13] Y. Shiraishi, N. Toshima, *Appl. Phys. Lett.* **2002**, *81*, 28457.

[14] W. Lee, C. Y. Wang, Y. C. Shih, *Appl. Phys. Lett.* **2004**, *85*, 513.

[15] B. Rozic, V. Tzitzios, E. Karatairi, U. Tkalec. G. Nounesis, Z. Kutnjak, G. Gordoyiannis, R. Rosso, E. G. Virga, I. Musevic, S. Kralj, *Eur. Phys. J. E* **2011**, *34*, 17.

[16] L. Wang, C. Zhao, F. Meng, S. Huang, X. Yuan, X. Xu, Z. Yang, H. Yang, *Colloids Surfaces A: Physicochem. Eng. Aspects* **2010**, *360*, 205.

[17] J. P. Sethna, *in Theory and Applications of Liquid Crystals* (Ed: J. L. Ericksen, D. Kinderlehrer) Springer-Verlag, New York, **1987**, p. 305.

[18] T. Iwata, K. Suzuki, N. Amaya, H. Higuchi, H. Masunaga, S. Sasaki, H. Kikuchi, *Macromolecules* **2009**, *42*, 2002.

[19] M. Ravnik, G. P. Alexander, J. M. Yeomans, S. Zumer, *Faraday Discuss.* **2010**, *144*, 159.

[20] J. Yan, H. C. Cheng, S. Gauza, Y. Li, M. Jiao, L. Rao, S. T. Wu, *Appl. Phys. Lett.* **2010**, *96*, 071105.

[21] L. Rao, J. Yan, S. T. Wu, S. Yamamoto, Y. Haseba, *Appl. Phys. Lett.* **2011**, *98*, 081109.

[22] a) K. M. Chen, S. Gauza, H. Xianyu, S. T. Wu, *J. Display Technol.* **2010**, *6*, 318; b) L. Rao, J. Yan, S. T. Wu, Y. C. Lai, Y. H. Chiu, H. Y. Chen, C. C. Liang, C. M. Wu, P. J. Hsieh, S. H. Liu, K. L. Cheng, *J. Display Technology* **2011**, *7*, 627; c) J. Yan, S. T. Wu, *J. Display Technol.* **2011**, *7*, 490.

[23] a) W. Helfrich, *Phys. Rev. Lett.* **1969**, *23*, 372; b) T. C. Lubenski, *Phys. Rev. A.* **1972**, *6*, 452; c) D. Marenduzzo, E. Orlandini, J. M. Yeomans, *Phys. Rev. Lett.* **2004**, *92*, 188301; d) A. Dupuis, D. Marenduzzo, E. Orlandini, J. M. Yeomans, *Phys. Rev. Lett.* **2005**, *95*, 097801.

[24] a) E. D. Palik, *Handbook of Optical Constants of Solids,* 1st ed., Academic, San Diego, **1985**, pp. 597–602; b) T. Joshi, A. Kumar, J. Prakash, A. M. Biradar, *Appl. Phys. Lett.* **2010**, *96*, 253109.